

# Stiffness and Buckling in Filament-Wound Motors

RICHARD RAVENHALL\*

*Hercules Powder Company, Rocky Hill, N. J.*

Development of stronger materials and improved fabrication techniques permit designers of filament-wound rocket motor cases to decrease wall thickness. As the walls become thinner, stiffness (resistance to bending deflection) and buckling become more critical. Design analyses and parametric curves for stiffness and buckling are presented. The buckling analysis uses Hess's equation for the buckling of orthotropic materials. The results are compared with existing test data, and a correction factor ( $k_c \sim 0.66$ ) for use with theoretical critical-compression buckling stresses is determined.

## Nomenclature

$A$	= area, in. <sup>2</sup>
$D$	= shell diameter, in.
$E$	= modulus of elasticity, lb/in. <sup>2</sup>
$G$	= shear modulus, lb/in. <sup>2</sup>
$I$	= shell moment of inertia, in. <sup>4</sup>
$k_c$	= compression buckling correction factor
$m$	= number of longitudinal buckling half-waves
$n$	= number of circumferential buckling waves
$P$	= longitudinal load, lb
$r$	= shell radius, in.
$R_D$	= rigidity ratio
$R_E$	= modulus ratio, $E_x/E_y$
$R_t$	= thickness ratio, $t/D$
$t$	= shell thickness, in.
$w$	= $\pi m$ , definition
$W_{max}$	= critical longitudinal load parameter
$\alpha$	= helix angle, deg
$\beta$	= see Eq. (A4), definition
$\delta$	= deflection, in.
$\epsilon$	= strain, in./in.
$\gamma$	= shearing strain, in./in.
$\mu$	= Poisson's ratio
$\sigma$	= stress, lb/in. <sup>2</sup>
$\tau$	= shearing stress, lb/in. <sup>2</sup>

## Subscripts

$f$	= glass filaments
$H$	= helical windings
$N$	= normal to filaments
$P$	= parallel to filaments
$r$	= resin
$x$	= longitudinal direction
$y$	= circumferential (hoop) direction
$zz$	= bending neutral axis
$90$	= hoop windings

## Introduction

FILAMENT-WOUND fiberglass, because it is light and strong, is now in use in a large number of rocket-motor case structures. For example, space and military motors with Spiralloy®† filament-wound fiberglass cases include the Altair and Antares used on the Scout missile, the Polaris second stage, the Minuteman third stage, and the Ranger retrorocket. The use of newer high-strength fiberglass, improved resins, and newly developed process techniques permit higher tensile stresses. The thinner rocket-case walls

made possible by these new developments are, however, more likely to be critical in stiffness (resistance to bending deflection) or in buckling. Optimum design will, accordingly, be increasingly dependent upon an understanding of the characteristics of the structure with regard to buckling and stiffness.

Nearly all filament-wound motors fabricated to date have employed the general type of winding structure and configuration illustrated in Fig. 1. Typically, glass filaments are first wound over a mandrel in a helical pattern at angles up to 45° with the motor axis. The helical windings extend over the cylindrical length and reverse over the domes. They are supplemented by hoop windings (at 90°) over the cylindrical length to give the two-to-one hoop-longitudinal strength required for internal pressure conditions. These glass filaments carry the primary load, while a resin binder, having a lower modulus of elasticity, carries and transmits secondary loadings to them. The resin also acts to create an over-all composite structure by eliminating relative strain between adjacent layers of filaments.

For calculating stiffness and buckling, the composite structure is treated as being orthotropic, that is, the elastic properties of the material are two-directional: along the longitudinal axis, and perpendicular to this axis (in the hoop direction). The stiffness of a given case, or its capability to resist bending deflections, is a function of its wall thickness and the longitudinal properties of the material. Calculation of buckling is more complex because it requires, in addition to wall thickness, consideration of the elastic properties in all directions. All of the elastic properties are definable by orthotropic relationships. In this paper design analyses for filament-wound fiberglass structures capable of withstanding high internal pressures and meeting stiffness and buckling requirements are discussed.

## Design Analysis

### Bending Stiffness

For a thin cylindrical filament-wound shell (Fig. 2) of radius  $r$  and thickness  $t$ , the bending stiffness (flexural rigidity) is given as

$$E_x I_{zz} = E_x \pi r^3 t \quad (1)$$

where the longitudinal modulus  $E_x$  will vary with the particular fiber orientation within the composite wall.

For an orthotropic material with its modulus of elasticity  $E_P$  parallel and  $E_N$  normal to its principal direction, the modulus at an intermediate angle  $\alpha$  is given by the relation<sup>1, 2</sup>

$$\frac{1}{E_\alpha} = \frac{\cos^4 \alpha}{E_P} + \frac{\sin^4 \alpha}{E_N} + \left[ \frac{1}{G_{PN}} - \frac{2\mu_{PN}}{E_P} \right] \sin^2 \alpha \cos^2 \alpha \quad (2)$$

This relation can also be taken for the special case of the longitudinal modulus of the helical windings, where these

\* Product Design Supervisor. Member AIAA.

Presented as Preprint 2904-63 at the AIAA Launch and Space Vehicle Shell Structures Conference, Palm Springs, Calif., April 1-3, 1963; revision received March 13, 1964. The author wishes to thank his colleagues J. P. Biro, R. A. Gere, and D. Pope for assistance during the preparation of this paper.

† Registered trademark by Hercules Powder Company for structures of oriented glass fiber and resin.

windings are at an angle  $\alpha$  to the longitudinal axis. For the usual filament-wound rocket-case design, an approximate form of Eq. (2) can be used to define the longitudinal and hoop moduli (see Appendix):

$$E_{Hx}^{-1} = E_P^{-1} \cos^2 \alpha + E_N^{-1} \sin^2 \alpha \quad (3)$$

$$E_{Hy}^{-1} = E_P^{-1} \sin^2 \alpha + E_N^{-1} \cos^2 \alpha \quad (4)$$

Since the wall is made up of a system of helical and hoop windings, each having a different modulus, the composite modulus can be written as a function of the two elastic constants,  $E_H$  and  $E_{90}$ :

$$E = E_{90} \{1 + (A_H/A) [(E_H/E_{90}) - 1]\} \quad (5)$$

Since the longitudinal modulus of the  $90^\circ$  windings is in the normal direction to the filaments, and the area of windings is proportional to the thickness, Eq. (5) becomes

$$E_x = E_N \{1 + (t_H/t) [(E_{Hx}/E_N) - 1]\} \quad (6)$$

and

$$E_y = E_P \{1 + (t_H/t) [(E_{Hy}/E_P) - 1]\} \quad (7)$$

where  $E_{Hx}$  and  $E_{Hy}$  are determined from Eqs. (3) and (4).

The solution of the previous relations can be achieved using either theoretical or test values for  $E_P$  and  $E_N$ . Theoretical values for  $E_P$  and  $E_N$  are determined using the following relations derived by Shaffer:<sup>3</sup>

$$E_P = E_r \{1 + (A_f/A) [(E_f/E_r) - 1]\} \quad (8)$$

$$E_N = E_r \{1 - (A_f/A) [1 - (E_r/E_f)]\}^{-1}$$

The following assumptions are typical for "E" glass and epoxy resin systems: 1) resin modulus,  $E_r = 5.0 \times 10^5$  lb/in.<sup>2</sup>; 2) glass filament modulus,  $E_f = 10.5 \times 10^6$  lb/in.<sup>2</sup>; and 3) approximately 65% filament by volume. These give  $E_P = 7.00 \times 10^6$  lb/in.<sup>2</sup>, and  $E_N = 1.57 \times 10^6$  lb/in.<sup>2</sup>; Figure 3 shows  $E_x$  and  $E_x/E_y$  (determined by Eqs. (6) and (7)) vs  $t_H/t$  for these values of  $E_P$  and  $E_N$  and with  $\alpha = 0^\circ$ ,  $15^\circ$ , and  $30^\circ$ . The values given here for  $E_x$  are applicable to the solution of bending stiffness (Eq. 1).

The usual procedure is first to determine the numbers of helical and hoop windings needed to satisfy over-all configuration and internal pressure conditions, and then to add windings, if necessary, to satisfy the stiffness requirement. The addition of only helical windings will increase the ratio of  $t_H/t$  and therefore will increase  $E_x$  and  $t$ . Studies of various specific situations have shown that it is possible to

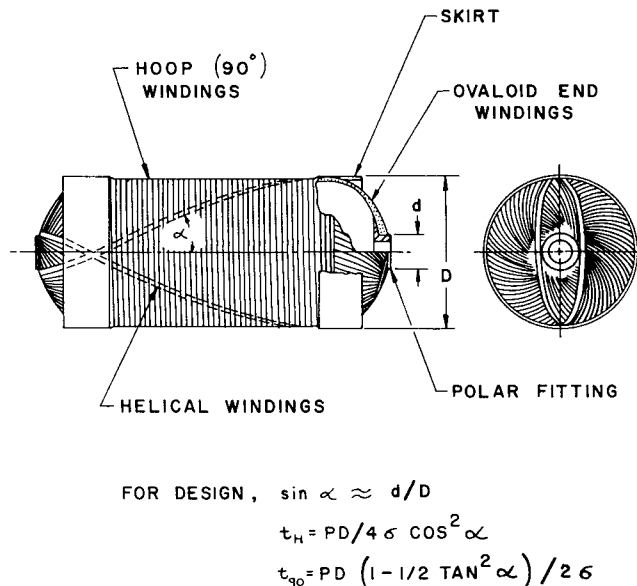


Fig. 1 Spiralloy filament-wound rocket case.

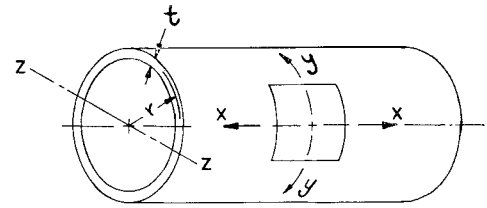


Fig. 2 Thin-walled cylindrical shell.

increase stiffness at about double the rate of increase of wall thickness.

### Buckling

The use of relations derived for the critical buckling stress in isotropic materials is not appropriate for filament-wound fiberglass structures, which, as previously noted, are orthotropic in nature, with properties that depend on the particular winding geometries employed. The parametric curves of Fig. 4 are determined using Hess's relation<sup>4</sup> for the critical longitudinal load parameter  $W_{\max}$  which takes into account the orthotropic nature of the material:

$$W_{\max} = (2P/\pi E_y D^2) (1 - \mu_{xy}^2 R_E^{-1}) = \eta/\xi \quad (9)$$

where

$$\eta = 2R_D R_E R_i w^4 + \frac{2}{3} R_i^3 [R_D R_E^2 w^2 + (4R_D^2 R_E + R_E) w^6 n^2 + 6R_D R_E w^4 n^4 + (R_E + 4R_D^2) w^2 n^6 + R_D n^8]$$

and

$$R_D = \text{rigidity ratio} = G_{xy} E_y^{-1} (1 - \mu_{xy}^2 R_E^{-1})$$

$$R_E \equiv E_x/E_y \quad R_i \equiv t/D \quad w \equiv m\pi$$

In the solution of Eq. (9), the mode shapes  $m$  and  $n$  are selected to give the minimum value of  $W_{\max}$  corresponding to any given shell geometry and material properties.

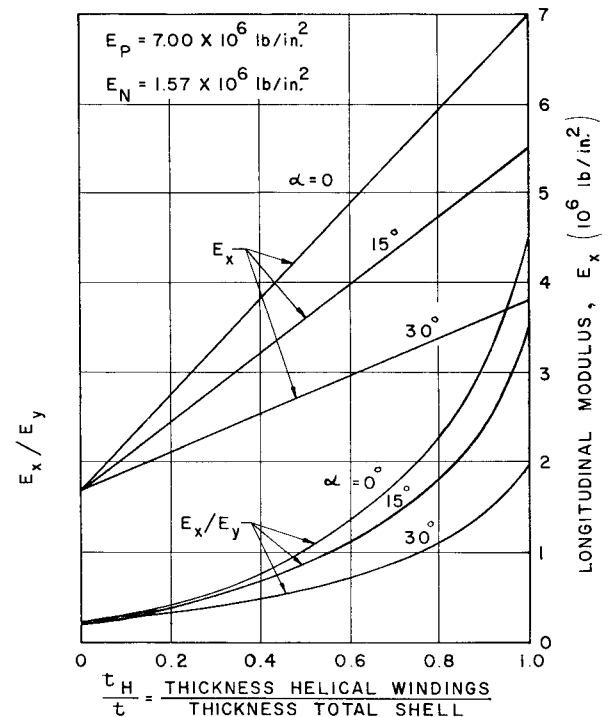


Fig. 3 Elastic moduli for a system of helical and hoop windings.

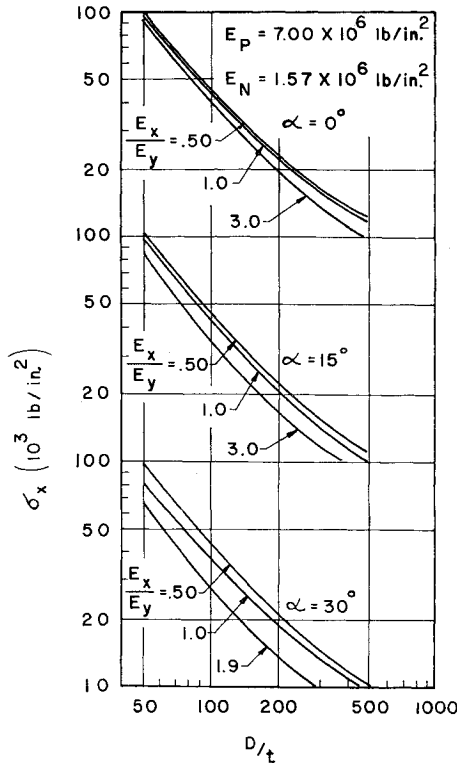


Fig. 4 Critical longitudinal buckling stress for system of helical and hoop windings.

To determine the critical stress in a cylindrical shell under uniform longitudinal loading let

$$\sigma_x = P/\pi Dt \quad (10)$$

Substituting for  $P$  from Eq. (9) into Eq. (10) and simplifying yields the relation for critical buckling stress:

$$\sigma_x = E_y W_{\max} [2R_t(1 - \mu_{xy}^2 R_E^{-1})]^{-1} \quad (11)$$

The solution of the foregoing equation requires values for the four elastic constants  $E_x$ ,  $E_y$ ,  $\mu_{xy}$ , and  $G_{xy}$  (for  $W_{\max}$ ). The elastic constants  $E_x$  and  $E_y$  are defined by Eqs. (6) and (7). Approximate values of  $\mu_{xy}$  are determined by letting  $\mu_{xy} E_x^{-1}$  equal a constant of  $5.15 \times 10^{-8}$ . This constant was determined from the average of measured values in Refs. 5 and 6. The shear modulus  $G_{xy}$  (see Appendix) is

$$G_{xy}^{-1} \approx E_x^{-1} + E_y^{-1} + 2\mu_{xy} E_x^{-1} \quad (12)$$

The rigidity ratio, Eq. (9), is determined by substituting for  $G_{xy}$  from Eq. (12). Rearranging terms gives

$$R_D = (R_E - \mu_{xy}^2)(R_E + 1 + 2\mu_{xy})^{-1} \quad (13)$$

The critical longitudinal load parameter  $W_{\max}$  is then defined by Eqs. (9) and (13) in terms of shell geometries and known structural properties, and the critical longitudinal stress  $\sigma_x$  is defined by Eq. (11) and  $W_{\max}$ . This stress is shown in Figs. 4 and 5 for various winding combinations,

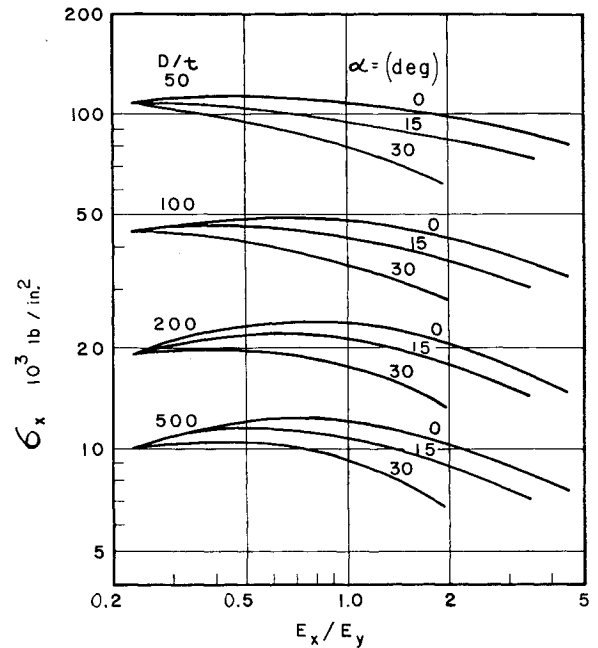


Fig. 5 Critical longitudinal buckling stress.

for the normal expected range of motor case geometries, and for material properties. A significant finding of the critical stress plots is that the maximum critical stress occurs at  $E_x/E_y \leq 1.0$  for all of the  $D/t$  values plotted. This confirms Hess's findings and shows that a high percentage of hoop windings in the composite gives the best buckling resistance. Thus, where it was found that the maximum improvement in bending stiffness is achieved with the addition of only helical windings, the buckling curves show that for maximum buckling improvement it is better to add hoop and helical windings, maintaining an  $E_x/E_y$  between 0.5 and 1.0.

### Test Correlation

A compression correction factor  $k_c$  for use in converting theoretical critical stresses  $\sigma_x$  to those expected in actual cases  $\sigma_x'$  is determined by comparing theoretical and test results. Results of one group of compressive buckling tests<sup>5</sup> conducted on 18-in.-diam, 30-in.-long Spiralloy tubes are summarized in Table 1. The tests consisted of compressing tubes having different numbers of layers of 15° and 90° windings. The stress developed  $\sigma_x'$  was not very sensitive to  $t_H/t$ , and  $k_c = \sigma_x'/\sigma_x$  fell in the range 0.63 to 0.69 for the four cases. Thus the averaged value,  $k_c = 0.66$ , should be useful for design. This compares with values of 0.40 to 0.60 for isotropic tubes.<sup>7</sup>

The buckling analysis used for compression is applicable, by analogy, to bending. An appropriate bending correction factor can also be determined by testing. Detailed design analysis of actual rocket cases will, of course, require consideration of many factors not covered in this study. These

Table 1 Compression buckling correction factor  $k_c$  for 18-in.-diam  $\times$  30-in.-long Spiralloy tubes with 15° helical windings

Averaged test data				Theoretical values			
Layers, 15°/90°	Wall thickness, $t$ , in.	$t_H$ $t$	Developed stress, $\sigma_x'$ , lb/in. <sup>2</sup>	$D$ $t$	$E_x$ $E_y$	Theo. stress, $\sigma_x$ , lb/in. <sup>2</sup>	$k_c = \frac{\sigma_x'}{\sigma_x}$
2/3½	0.059	0.35	10,160	304	0.62	15,500	0.655
3/3	0.070	0.50	10,920	257	0.83	17,400	0.630
4/2	0.073	0.67	11,630	246	1.26	17,000	0.685
5/1	0.074	0.83	10,460	243	1.93	15,200	0.688

must include the specific properties of the particular resin and glass system, the final expected resin content, and other process parameters.

### Appendix

The following analysis represents a simplified approach for defining the elastic properties of an orthotropic material which are needed for stiffness and buckling calculations. The relations derived can be used to define the elastic properties of the helical windings in most filament-wound rocket cases loaded uniaxially.

#### Shear Modulus

A block of orthotropic material, with moduli  $E_P$  and  $E_N$  in the directions parallel and normal to its principal direction, and with its principal strength in a direction having an angle  $\alpha$  to the  $x$  direction, is considered to be under equal tensile and compressive forces, as shown in Fig. 6.<sup>8</sup> Pure shear will

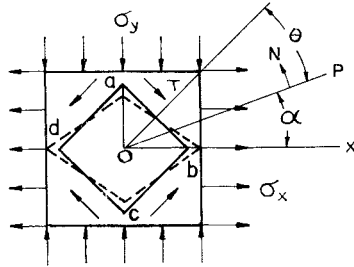


Fig. 6 Model for shear modulus.

exist along the surfaces of element  $abcd$ , and the shear deflection will be a measure of the shear modulus at an angle  $45^\circ$  to the  $x$  direction or at an angle  $\theta$  ( $\theta = 45^\circ - \alpha$ ) to the direction of the principal material strength. The strain relations in the  $x$  and  $y$  directions are

$$\epsilon_y = \sigma_y E_y^{-1} - \mu_{xy} \sigma_x E_x^{-1}$$

$$\epsilon_x = \sigma_x E_x^{-1} - \mu_{xy} \sigma_y E_y^{-1}$$

To establish the relationship of  $\epsilon_y$  to  $\epsilon_x$  when  $\sigma_x = -\sigma_y$ , consider the triangle  $oab$  in Fig. 7, where  $\gamma$  = distortion of element  $abcd$  = shearing strain. From this, for a small angle  $\gamma$ ,

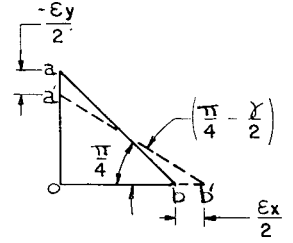
$$\tan\left(\frac{\pi}{4} - \frac{\gamma}{2}\right) = \frac{oa'}{ob'} = \frac{1 + \epsilon_y}{1 + \epsilon_x} \approx \frac{1 - (\gamma/2)}{1 + (\gamma/2)}$$

Also, for the condition of pure shear,  $\sigma_x = -\sigma_y = \tau$ , and from Maxwell's reciprocal theorem,  $\mu_{xy} E_x^{-1} = \mu_{yx} E_y^{-1}$ . By definition, the shear modulus is  $G_\theta = \tau/\gamma$ . These relations can be combined to give

$$\begin{aligned} G_\theta^{-1} &= E_x^{-1} + E_y^{-1} + 2\mu_{xy} E_x^{-1} + (\gamma/2)(E_y^{-1} - E_x^{-1}) \\ &\approx E_x^{-1} + E_y^{-1} + 2\mu_{xy} E_x^{-1} \end{aligned} \quad (A1)$$

The elastic modulus at an angle  $\alpha$  to the principal direction is given by Eq. (2)<sup>1</sup>,<sup>2</sup> in the main text, which gives the elastic moduli in the  $x$  and  $y$  directions:

Fig. 7 Relationship of  $\epsilon_y$  to  $\epsilon_x$  when  $\sigma_x = -\sigma_y$ .



$$E_x^{-1} = \cos^4 \alpha E_P^{-1} + \sin^4 \alpha E_N^{-1} + \beta \quad (A2)$$

$$E_y^{-1} = \sin^4 \alpha E_P^{-1} + \cos^4 \alpha E_N^{-1} + \beta \quad (A3)$$

Substituting Eqs. (A2) and (A3) into (A1) gives

$$\begin{aligned} G_\theta^{-1} &= (E_P^{-1} + E_N^{-1})(\cos^4 \alpha + \sin^4 \alpha) + \\ &\quad 2\mu_{xy} E_x^{-1} + 2\beta \end{aligned} \quad (A4)$$

where  $\beta \equiv \sin^2 \alpha \cos^2 \alpha [G_{PN}^{-1} - 2\mu_{PN} E_P^{-1}]$ .

Collected data for filament-wound rocket-case structures (helix angles  $0^\circ$ – $30^\circ$ ) indicate that  $\mu_{xy} E_x^{-1}$  can be approximated by a constant. Therefore, letting  $\mu_{PN} E_P^{-1} = \mu_{xy} E_x^{-1}$ ,

$$\begin{aligned} G_\theta^{-1} &\approx (E_P^{-1} + E_N^{-1} + 2\mu_{PN} E_P^{-1}) \times \\ &\quad (1 - 2 \sin^2 \alpha \cos^2 \alpha) + G_{PN}^{-1} (2 \sin^2 \alpha \cos^2 \alpha) \\ &\approx E_P^{-1} + E_N^{-1} + 2\mu_{PN} E_P^{-1} = \text{a constant} \end{aligned} \quad (A5)$$

Since the shear-modulus term is here taken to be a constant, it is possible to approximate the shear modulus by Eq. (12) in the main text.

#### Elastic Moduli

Approximate elastic-moduli relations can be determined by substituting for  $G_{PN}$  in Eqs. (A2) and (A3) to give Eqs. (3) and (4) in the main text.

#### References

- Love, A. E. H., *A Treatise on the Mathematical Theory of Elasticity* (Dover Publications, New York, 1944), 4th ed., pp. 161, 162.
- Sonneborn, R. H., *Fiberglass Reinforced Plastics* (Reinhold Publishing Corp., New York, 1954), pp. 181–188.
- Shaffer, B. W., "The stress-strain relations of Spiralloy with filaments parallel or normal to the applied force," Hercules Powder Co., HPC-050-12-1-1 (June 1961).
- Hess, T. E., "Stability of orthotropic cylindrical shells under combined loading," *ARS J.* **31**, 237–246 (1961).
- Sargent, T. V., "Compressive testing of eighteen-inch i.d. Spiralloy cylinders," Hercules Powder Co., Rept. MTI-123 (February 1960).
- Sargent, T. V., "A study of environmental storage effects on the strength of Spiralloy," Hercules Powder Co., Rept. MTO-125 (July 1961).
- Roark, R. J., *Formulas for Stress and Strain* (McGraw-Hill Book Co., Inc., New York, 1954), 3rd ed., p. 316.
- Timoshenko, S., *Strength of Materials—Part I* (D. Van Nostrand Co., Inc., Princeton, 1958), 3rd ed., pp. 53–61.